INVESTIGATION INTO THE RELIABILITY OF PREDICTIVE PORE-SCALE MODELING FOR SILICICLASTIC RESERVOIR ROCKS

Olivier Lopez[1], Alexander Mock[1], Jostein Skretting[2], Egil Boye Petersen Jr. [2], Pål-Eric Øren[1] , Alf Birger Rustad[2]
[(1)]NumericalRocks AS and [(2)]Statoil ASA

This paper was prepared for presentation at the International Symposium of the Society of Core Analysts held in Halifax, Nova Scotia, Canada, 4-7 October, 2010

ABSTRACT

The prediction of petrophysical and multiphase flow properties from direct pore-scale modeling has received a lot of attention in recent years. Although successful results have been reported for a number of outcrop and reservoir rocks, no exhaustive study has been performed to verify the consistency of such predictions across a wide range of rocks. Consequently, uncertainties prevail about the reliability of pore-scale modeling results for complex rocks such as those encountered in the petroleum industry. In the present work, an integrated pore-scale modeling approach was applied to 28 siliciclastic reservoir rock samples from six different fields and seven different formations from the Norwegian continental shelf (NCS). The reservoir rocks have a clay fraction of up to 0.19 and well to moderately sorted grain size distributions. The samples span almost four orders of magnitude in permeability (5mD to 20D) and nearly three decades of porosity (0.14 to 0.43). For each sample, a 3D model of the rock was constructed based on thin section analysis and geological process based modeling. Conventional and special core analysis data were available and considered during the modeling process. Predicted petrophysical properties include porosity and absolute permeability. Absolute permeability was computed using Lattice-Boltzmann simulations. Primary drainage and waterflood relative permeabilities were determined from two-phase oil-water flow simulations on the pore network representation of the 3D rock model. Flow simulation input parameters were set according to expected wettability conditions. The predicted results are compared with a large number of measured data obtained by different experimental methods and with observed field trends. Very good agreement is obtained between pore-scale modeling derived properties and available experimental data throughout the studied data set. Computed results also capture observed cross-property correlations, such as porosity vs. permeability and end point relative permeability vs. residual saturation. Deviations from the experimental data are explained in terms of sample heterogeneity, detailed pore-scale observations, and reliability of the experimental method. It is concluded that the applied integrated pore-scale modeling approach yields reliable and consistent data for siliciclastic rocks within the investigated porosity (0.14 to 0.43) and permeability (5mD to 20D) range and under weakly water-wet to weakly oil-wet conditions.

INTRODUCTION

In oil and gas exploitation, Conventional and Special Core Analyses (CCA and SCAL) are crucial for reservoir description and simulation. These procedures are relatively time consuming and are applied on a very small number of drilled cores. Pore scale modeling can add significant value, as it can extend a small experimental dataset on the basis of 2D or 3D images on a much shorter timescale. In recent years there has been an explosion of interest in pore-scale modeling and promising results have been reported for a number of complex porous rocks (Adler *et al.*, 1990; Caubit *et al*., 2008; Cense *et al.*, 2008; Touati *et al.*, 2009). But no exhaustive study has been performed to verify the consistency of such predictions across a wide range of siliciclastic rocks and to validate a pore scale modeling approach to acquire reliable data for reservoir description and simulation. The aim of this study was to establish an operational range (porosity, permeability, clay content etc.) for pore scale modeling using the commercial software eCore. This includes rock modelling, calculation of petrophysical properties, 2-phase fluid flow simulations and comparison of predicted results with laboratory data for water/oil system. In the present work completed within 3 months, an integrated pore-scale modeling approach was used to reconstruct 28 siliciclastic reservoir rock samples from six different fields and seven different formations from the NCS. The reconstructed reservoir rocks have well to moderately sorted grain size distributions and a clay fraction of up to 0.19. The sample permeabilities span four orders of magnitude (5mD to 20D) and the porosity of the samples varies from 0.14 to 0.43. On these 28 samples, oil/water flow simulations for drainage and imbibition have been performed to estimate capillary pressure and relative permeabilities. The results from simulations are compared with a large collection of relevant CCA and SCAL data and with observed field trends.

METHODOLOGY

Pore Scale Reconstruction of Reservoir Rocks

Numerical 3D sandstone reservoir rock models have been constructed based on thin section analysis and by simulating geological rock forming processes: sedimentation, compaction, and diagenesis. For each sample, three model realizations are generated and their input parameters are varied in order to reflect variation observed in available rock data on the thin section and plug scale. The three realizations are then used for all the single phase and 2-phase calculations and results are reported as mean value for each reconstructed sample. The models are thus discrete models in themselves and not perturbations of a single master model. Variation in result data reflects the expected variation of petrophysical and reservoir properties at the pore and core scale. Thin sections were imaged with a backscattered scanning electron microscope (BSEM). Resulting images are segmented into binary images of porosity, clay minerals, grain matrix and cementing minerals. Grain sizes are extracted by a distance transform and maximum inscribed circle algorithm applied on the grain matrix images. An empirical

correlation is applied to correct for stereological effects (Øren and Bakke, 2002). The fraction of clay minerals is corrected for partial volume effects by applying a granulometric filter (Prodanov *et al.*, 2005). Results of BSEM image analysis are used in the modeling routine. Conventional and special core analysis data were available and considered during the modeling process, but are not used as input parameters to the modeling routine. Process based models are compared visually to thin section images. All 3D rock images used for further calculation have representative elementary volumes (REV). 3D rock images are statistically similar to thin section images. Predicted petrophysical properties include porosity and absolute permeability. Porosity is obtained from BSEM image analysis (intergranular porosity) and a model for sub-resolution microporosity (total porosity). Absolute permeability was computed using Lattice-Boltzmann simulations (Øren *et al.*, 2006, Jin et al. 2004).
The reconstructed rock models were simplified into pore network models. Crucial geometrical and topological properties were retained, while the data volume is reduced to allow timely computation (Øren and Bakke, 2003). Since the extracted pore network is in a one-to-one correspondence with the reconstructed pore space, no fitting or tuning parameters are introduced to match macroscopic parameters such as porosity and permeability. In pore network modelling, local capillary equilibrium and the Young–Laplace equation are used to determine multiphase fluid configurations for any pressure difference between phases for pores of different shape and with different fluid/solid contact angles. The pressure in one of the phases is allowed to increase and a succession of equilibrium fluid configurations are computed in the network. Then, empirical expressions for the hydraulic conductance of each phase in each pore and throat are used to define the flow of each phase in terms of pressure differences between pores. Conservation of mass is invoked to find the pressure throughout the network, assuming that all the fluid interfaces are frozen in place. From this the relationship between flow rate and pressure gradient can be found and hence macroscopic properties, such as absolute and relative permeabilities, can be determined. The following displacements were simulated on the extracted pore networks of the reconstructed models: oil/water primary drainage to initial water saturation S_{wi}, and waterflooding to residual oil saturation S_{or}. At the pore scale, it is assumed that the displacement processes are quasi-static and capillary dominated. This is a reasonable assumption for low capillary number processes that are typical of most reservoir displacements. The input parameters for the wettability modeling were set according to expected wettability conditions based on available SCAL results. The predicted results are compared with a large number of measured data obtained by different experimental methods and with observed field trends.

Experimental data

All available conventional and special core analysis data from the modeled fields have been considered during this study. The use of laboratory results is twofold. Conventional data, such as porosity, permeability, grain density, XRD and thin sections are evaluated

alongside primary drainage capillary pressure data to ensure the rock models represent the actual core material. Wettability and oil/water relative permeability data are used to identify the expected wettability conditions to be used in the flow simulations and to evaluate the quality of the simulation predictions. The predicted results are compared to results from neighboring plugs. In addition CCA and SCAL datasets are used to compare the predictions and trends at several levels, e.g. well level, field level and formation at field or NCS level. The dataset consists of scalars from quality controlled dynamic experiments. In this study the most relevant experiments are Amott/USBM tests, single speed centrifuge, unsteady state and steady state waterfloods. The scalars used are S_{wi}, S_{or}, water relative permeability at residual oil saturation ($k_{rw}(S_{or})$) and Corey and LET representation of analytical and history matched relative permeability curves. The database approach is useful to ensure a consistent and robust description of the laboratory achieved flow properties. Relative permeability recommendations are divided into base, low and high cases to capture the spread of data for each field. For quality evaluation of predicted results, it is important to filter the data with respect to experimental method and conditions. Generally, S_{or} and $k_{rw}(S_{or})$ from centrifuge experiments and Corey/LET parameters from steady state waterflood are considered more reliable.

RESULTS AND DISCUSSION

Very good agreement is obtained between pore-scale modeling derived properties and available experimental data throughout the studied data set (porosity between 0.14 and 0.34, permeability <5D). Porosity and permeability data were compared to conventional core analysis data available for each field. Computed results also capture field specific observed cross-property correlations, such as porosity vs. permeability (Figure 1), S_{wi} vs. permeability (Figure 2) and end-point relative permeability vs. residual saturation (Figure 3). Table 1 gives an overview of predicted results for all samples. Field 6 was an exception. In this case, relative permeability curves were compared to results of steady state and centrifuge experiments performed on a representative sample. Predicted relative permeability curves for the 28 samples were compared to available recommendations (figure 4). The water saturation (S_w) has been normalized (S_{wN}) with respect to initial water saturation as:

$$S_{wN} = \left(\frac{S_w - S_{wi}}{1 - S_{wi}} \right) \quad (1)$$

Below, results are discussed field by field.

Field 1

Three samples from one formation were selected from field 1. The porosity range is from 0.14 to 0.17; permeabilities range from 40mD to 200mD. In terms of porosity, permeability and S_{wi}, all model results fall within the range of experimental data. These results also follow the same general field trends as observed in Figures 1 and 2. Based on evaluation of all available SCAL data, weakly oil-wet or neutral wettability conditions were proposed. The average Amott index obtained from the simulations is -0.19 (weakly

oil-wet). Simulated oil relative permeabilities for the three samples have been compared to field recommendations. They follow the low case recommendation, whereas the water relative permeability matches well with the base case recommendation (Figure 4). End point relative permeability vs. residual saturation resulting from the simulations is in very good agreement with the available dataset for this field (Figure 3).

Field 2

Five samples from two different formations were considered from field 2; two samples have high fraction of clay. All simulated results fall inside the experimental data range and follow the trend of experimental data available for the same well. Porosities range from 0.23 to 0.32, permeabilities from 50mD to almost 3D. Based on evaluation of all available SCAL data, neutral or weakly water-wet wettability conditions were proposed for simulations. The average resulting Amott index for the simulations is around 0 indicating mixed wet conditions. Simulated relative permeability curves are aligned with the base case recommendation for the field. End-point relative permeability vs. residual saturation resulting from the simulations is in very good agreement with the available dataset for this field.

Field 3

Four samples from two different formations were considered from field 3. All samples have very high porosity (>0.35) and permeability (up to 20D). No saturation measurements were available for these samples. The simulated results match conventional core analysis data for similar depths very well in terms of porosity and permeability. Flooding experiments could not be carried out on these plugs due to their fairly unconsolidated state and very high permeability and porosity. Comparison has been made with available experiments on plugs with the closest porosity permeability ratio. S_{orw} values from simulations are in the same range as achieved in centrifuge experiments. Based on evaluation of all available SCAL data, medium to strongly water-wet wettability conditions were proposed for simulations. The average resulting Amott index for the simulations is 0.59. Relative permeability recommendations are based on lower permeability/porosity samples. Simulated water relative permeabilities for the four samples are in good agreement with the high case of relative permeability recommendations for this field, whereas simulated oil relative permeabilities follow the base case. It is expected that higher permeability and porosity of the reconstructed samples tend to lift up the water relative permeability as during a drainage process.

Field 4

Three samples from one formation have been included from field 4. These cover a range in porosity from 0.14 to 0.24 and a range in permeability from 25mD to 600mD. All simulated results fall within the range shown by special core analysis data and conventional core analysis for the entire field. Field trends are captured in terms of porosity-permeability correlations and correlations with S_{wi}. Based on evaluation of all available SCAL data, weakly oil-wet or neutral wettability conditions were proposed. The average Amott index yielded in simulations is -0.23 and is on the lower side of the

recommendation for this formation. Simulated water relative permeabilities for the samples match the recommended base case, oil relative permeability curves follow the base case or the low case recommendation for normalized water saturation with respect to S_{wi}. End-point relative permeability vs. residual saturation resulting from the simulations is in very good agreement with the available dataset for this field.

Field 5

Eight samples were considered from two different formations from field 5. All samples from formation two have a high fraction of clay. Total measured sample porosity ranges from 0.28 to 0.35. Permeability of the formation one samples is around 2D, whereas the formation two samples range from 500mD to 700mD. All simulated results fall within the range and follow the same trend as suggested by available experimental data. This field has been studied well by traditional core analysis. The results from the simulations fall well within the experimental data range and follow the same trends of almost 50 different SCAL data. Based on evaluation of all available SCAL data, neutral or weakly water-wet wettability conditions were proposed. Simulations yield an average Amott index of 0.1. Base case relative permeability SCAL recommendations for the two formations in this field are very similar for both water and oil relative permeability. Simulated relative permeabilities are in very good alignment with the recommended curves.

Field 6

Five samples from one formation have been selected from field 6. These samples show a high degree of cementation and a wide range in pore sizes mainly due to secondary porosity (grain dissolution). Porosity ranges from 0.14 to 0.19; permeability from 5mD to 500mD. Where experiments are available for modeled plugs, simulated results are very close to laboratory data. Two of the samples are challenging in terms of high fraction of clay and low porosity and contain more numerical uncertainties, but all simulated results fall within the range of experimental data and follow the same trends. No relative permeability recommendations are available for field 6 at the moment. Based on evaluation of all available SCAL data, weakly oil-wet wettability conditions were proposed. The average Amott index obtained from simulations is -0.10. End-point relative permeability vs. residual saturation resulting from the simulations is in very good agreement with the available dataset for this field.

CONCLUSION

For the six investigated fields, the single phase properties (porosity and permeability) from the reconstructed samples are in very good agreement with the experimental data available for each field and follow the observed trends. For the two phases (oil/water) flow simulation, the relative permeability end points and the achieved residual oil and water saturation are comparable to the available data and also show trends similar to the ones observed for each field.

It is concluded that the applied integrated pore-scale modeling approach yields reliable and consistent data for siliciclastic rocks within the investigated porosity (0.14 to 0.43) and permeability (5mD to 20D) range and under weakly water-wet to weakly oil-wet conditions. The combination of conventional or special core analysis and applied integrated pore-scale modeling demonstrates the capability of extending existing data set in a short time frame of three months and in a reliable manner.

ACKNOWLEDGEMENTS

This study was part of a Statoil internal project and the authors would like to thank Statoil for permission to publish this work.

REFERENCES

1. Touati, M., Suicmez, S., Funk, J., Cinar, Y. and Knackstedt, M., “Pore Network Modeling of Saudi Aramco Rocks: A Comparative Study” SPE paper 126043, presented at SPE Saudi Arabia Section Technical Symposium and Exhibition, Al Khobar, May 2009.
2. Øren, P.E. and Bakke, S., "Reconstruction of Berea Sandstones and Pore-Scale Modeling of Wettability Effects", J. Petroleum Science & Engineering, 2003, 39, 177-199.
3. Øren, P.E., Bakke, S. and Arntzen, O.J., "Extending Predictive Capabilities to Network Models", SPEJ, 1998, 324-336.
4. Øren, P.E. and Bakke, S., "Process Based Reconstruction of Sandstones and Prediction of Transport Properties", Transport in Porous Media, 2002, 46, 311-343.
5. Adler, P.M., Jacquin, C.G. and Quiblier, J.A., “Flow in simulated porous media”, International Journal of Multiphase Flow, 1990, 16: 691-712.
6. Caubit, C., Hamon, G., Sheppard, A.P. and Øren, P.E. “Evaluation of the reliability of prediction of petrophysical data trough imagery and pore network modelling“, Proceedings of the Annual Symposium of the Society of Core Analysts, SCA2008-33, Abu Dhabi, United Arab Emirates.
7. Cense, A. and Marcelis, F. “A comparative study of three pore-scale reconstruction and pore-network extraction technique“, Proceedings of the Annual Symposium of the Society of Core Analysts, SCA2008-36, Abu Dhabi, United Arab Emirates.
8. Prodanov, D., Heeroma, J. and Marani, E., “Automatic morphometry of synaptic boutons of cultured cells using granulometric analysis of digital images”, Journal of Neuroscience Methods, 2006, 151, 168-177.
9. Jin, G., Patzek, T.W. and Silin, D.B., “Direct Prediction of Absolute Permeability of Unconsolidated and Consolidated Reservoir Rock”, SPE paper 90084, presented at the SPE ATCE, Houston, TX, September 2004.

10. Øren, P.E., Bakke, S. and Rueslåtten, H.G., "Digital Core Laboratory: Rock and Flow Properties Derived from Computer Generated Rocks", SCA2006-21, Trondheim, Norway.

Table 1: Predicted results from simulations for the 28 samples (3 realizations per sample)

Field	Sample ID	Porosity (frac)	Permeability (mD)	S_{wi} inital water saturation (frac)	Amott Harvey wettability index	S_{orw}	$k_{rw}(S_{orw})$	Clay cont. (frac)
1	1A	0.154	148.0	0.08	-0.16	0.13	0.76	0.0181
1	1B	0.155	86.0	0.12	-0.20	0.17	0.74	0.033
1	1C	0.154	49.0	0.13	-0.22	0.19	0.68	0.0249
2	2A	0.255	169.1	0.15	0.03	0.12	0.82	0.0504
2	2B	0.261	373.8	0.13	-0.06	0.10	0.86	0.0526
2	2C	0.301	742.2	0.125	-0.05	0.09	0.90	0.0782
2	2D	0.244	74.5	0.27	-0.04	0.15	0.74	0.1053
2	2E	0.291	2759	0.21	0.12	0.14	0.80	0.1084
3	3A	0.412	17787	0.06	0.54	0.14	0.72	0.0464
3	3B	0.386	11243	0.05	0.57	0.15	0.67	0.0358
3	3C	0.373	3000	0.06	0.58	0.15	0.64	0.0405
3	3D	0.375	1204	0.1	0.65	0.19	0.50	0.0714
4	4A	0.174	57.1	0.3	-0.31	0.16	0.60	0.0895
4	4B	0.239	246	0.24	-0.17	0.11	0.87	0.099
4	4C	0.144	103.8	0.2	-0.22	0.14	0.70	0.045
5	5A	0.326	1100	0.18	0.08	0.16	0.70	0.1352
5	5B	0.344	1320	0.2	0.10	0.17	0.67	0.106
5	5C	0.326	527.7	0.165	-0.02	0.14	0.80	0.156
5	5D	0.312	572.5	0.17	-0.05	0.14	0.80	0.1616
5	5E	0.319	538	0.176	-0.01	0.14	0.79	0.1717
5	5F	0.329	491	0.27	0.17	0.14	0.76	0.2579
5	5G	0.298	513	0.25	0.20	0.15	0.71	0.1633
5	5H	0.299	424	0.18	0.22	0.18	0.66	0.2182
6	6A	0.183	96.9	0.17	-0.14	0.13	0.75	0.0516
6	6B	0.160	22.0	0.27	-0.20	0.12	0.73	0.0833
6	6C	0.142	368	0.29	-0.06	0.15	0.62	0.08
6	6D	0.176	14.8	0.1	-0.14	0.10	0.82	0.0367
6	6E	0.177	522	0.07	0.03	0.07	0.87	0.0217

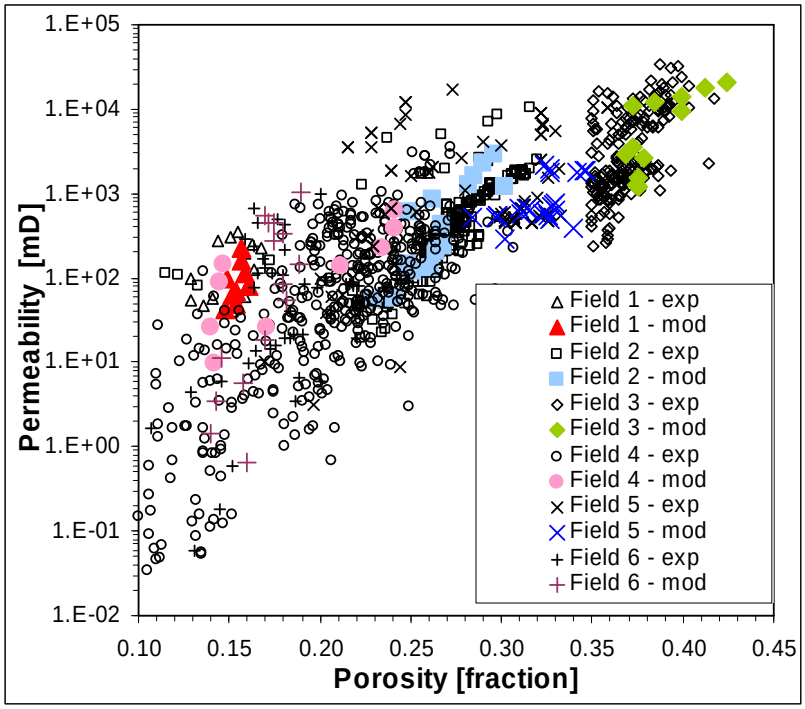

Figure 1: Cross plot of porosity (fraction) as a function of permeability (in mD) for simulated (mod) and laboratory (exp) experiments.

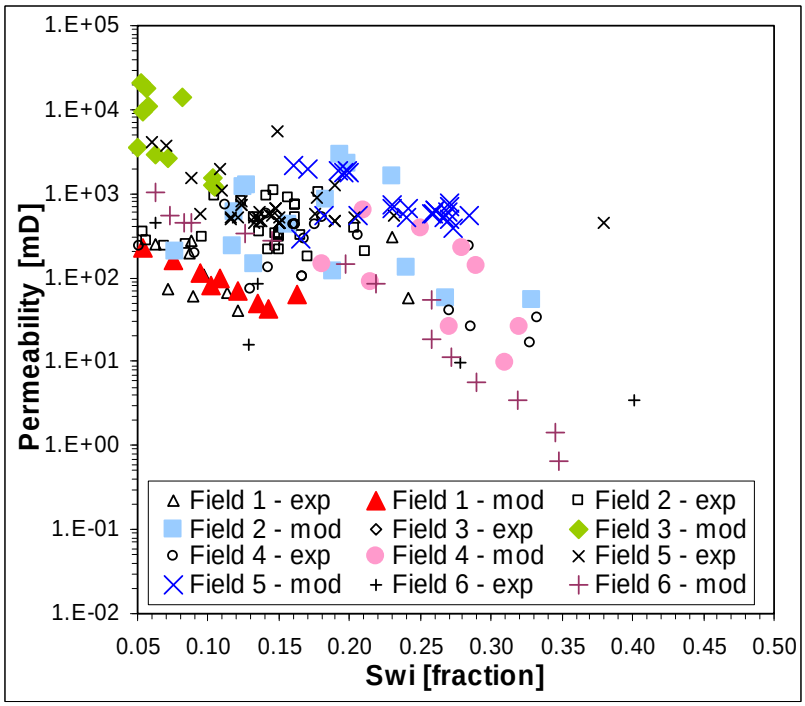

Figure 2: Cross plot of initial water saturation (S_{wi}) as a function of permeability (in mD) for simulated (mod) and laboratory (exp) experiments.

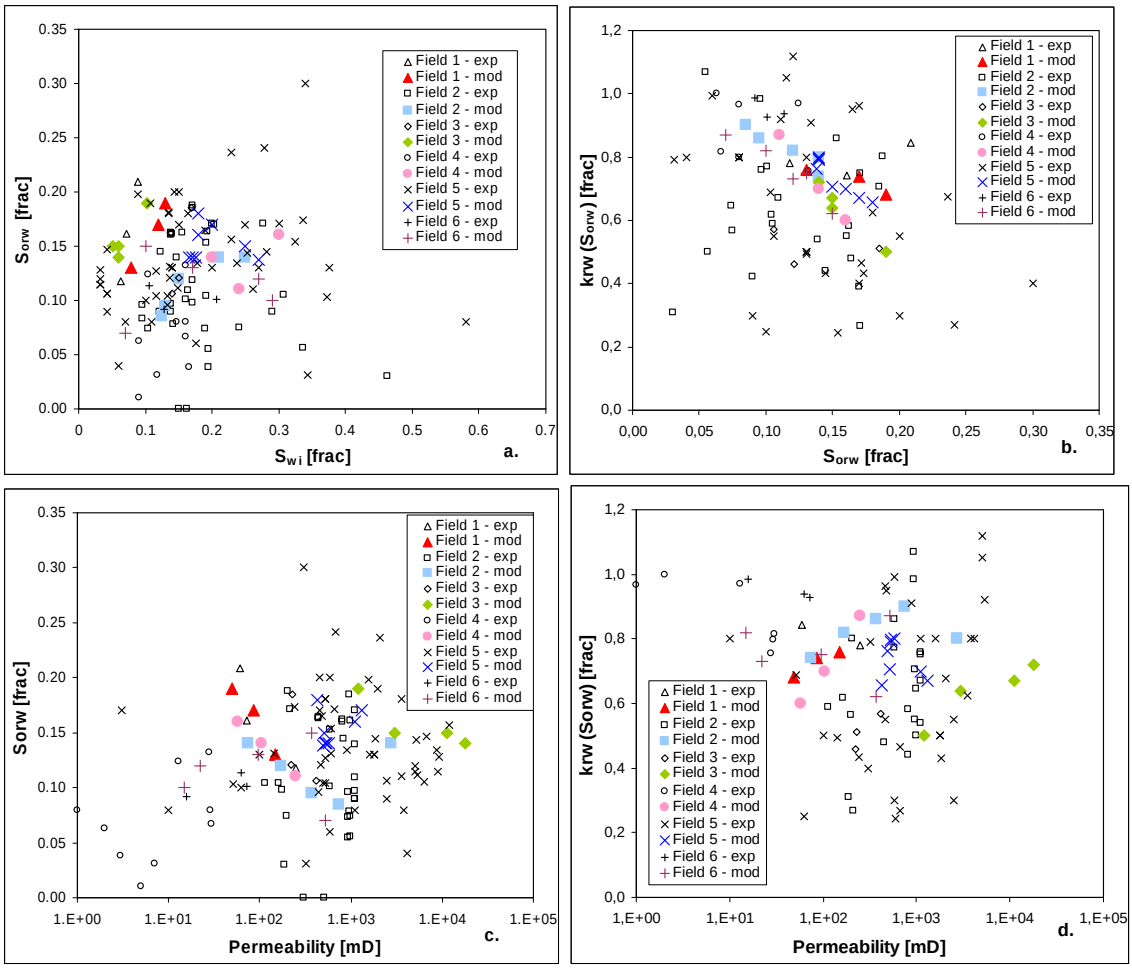

Figure 3: Multiphase flow cross plots for all the investigated fields
a. initial water saturation (S_{wi}) vs. residual oil saturation after waterflooding (S_{or}); b. S_{orw} vs. water relative permeability at S_{orw} ($k_{rw}@S_{orw}$); c. S_{orw} vs. permeability (k in mD); d. $k_{rw}@S_{orw}$ vs. permeability (k in mD).

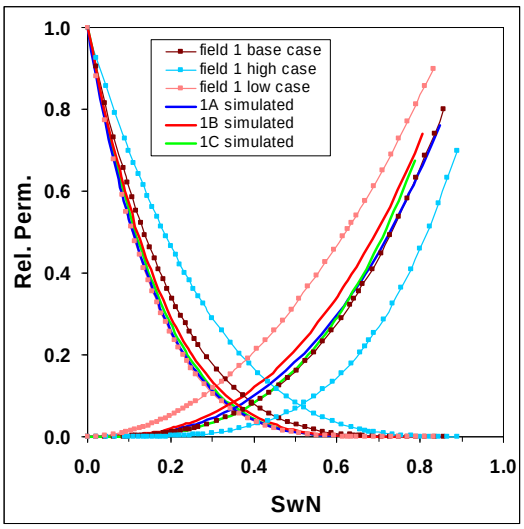
Rel. Perm.
SwN
field 1 base case
field 1 high case
field 1 low case
1A simulated
1B simulated
1C simulated

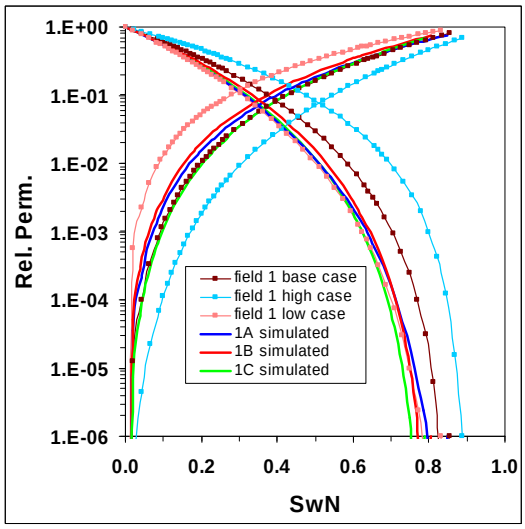
Rel. Perm.
SwN
field 1 base case
field 1 high case
field 1 low case
1A simulated
1B simulated
1C simulated

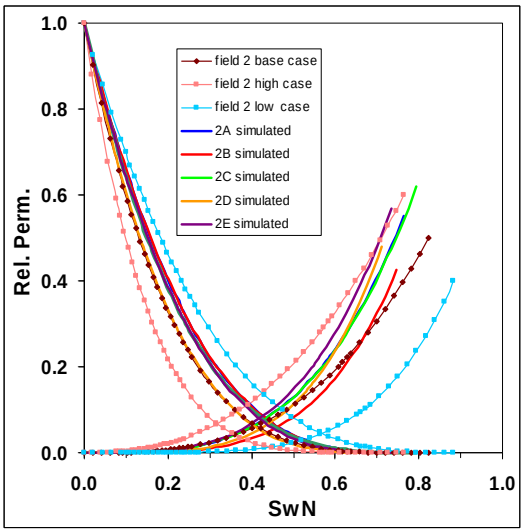
Rel. Perm.
SwN
field 2 base case
field 2 high case
field 2 low case
2A simulated
2B simulated
2C simulated
2D simulated
2E simulated

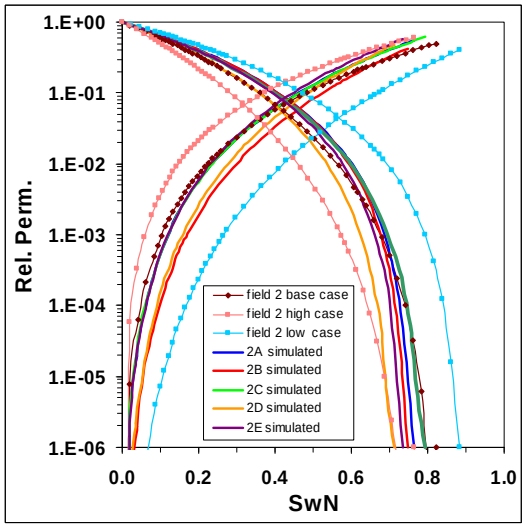
Rel. Perm.
SwN
field 2 base case
field 2 high case
field 2 low case
2A simulated
2B simulated
2C simulated
2D simulated
2E simulated

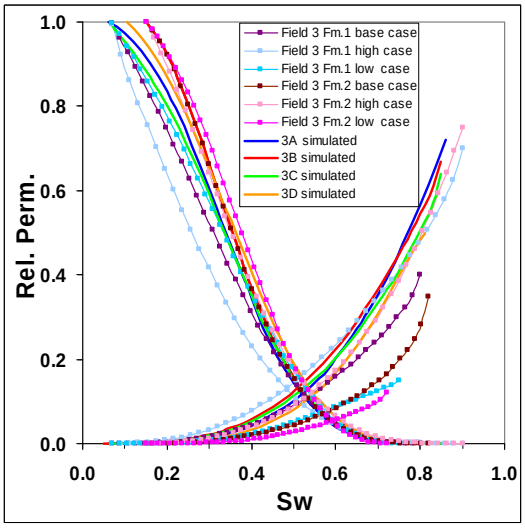
Rel. Perm.
Sw
Field 3 Fm.1 base case
Field 3 Fm.1 high case
Field 3 Fm.1 low case
Field 3 Fm.2 base case
Field 3 Fm.2 high case
Field 3 Fm.2 low case
3A simulated
3B simulated
3C simulated
3D simulated

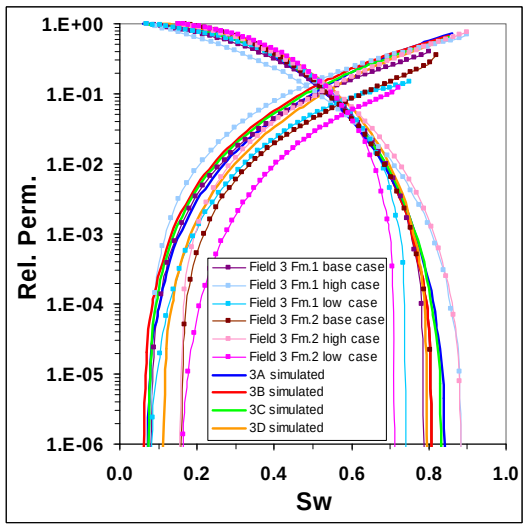
Rel. Perm.
Sw
Field 3 Fm.1 base case
Field 3 Fm.1 high case
Field 3 Fm.1 low case
Field 3 Fm.2 base case
Field 3 Fm.2 high case
Field 3 Fm.2 low case
3A simulated
3B simulated
3C simulated
3D simulated

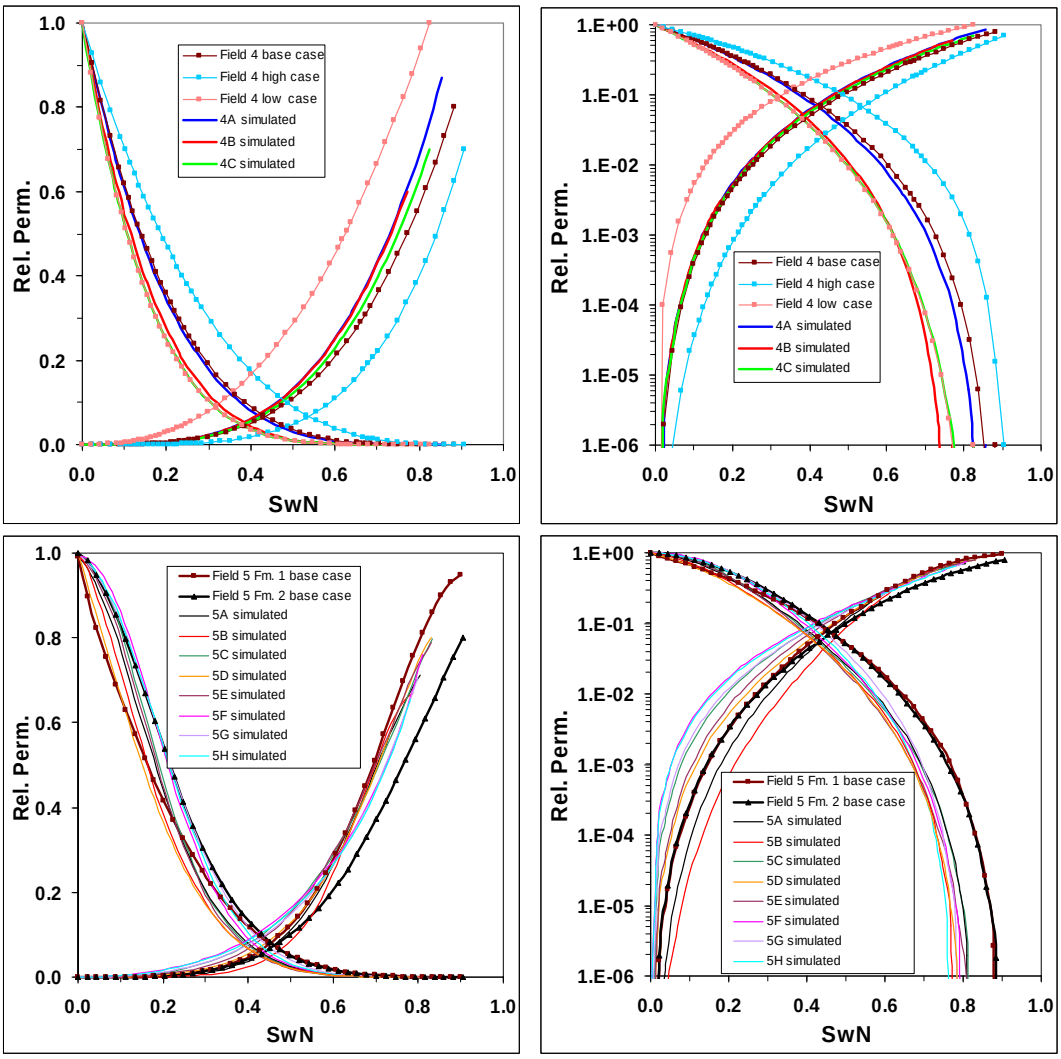

Figure 4: Comparison of recommended imbibition relative permeability (Corey fitted) vs. normalized water saturation (S_{wN}) between field recommendations (dotted lines) and resulting from flow simulations (plain lines) for all the 6 investigated field.